Supporting Information

Charge-Delocalized State and Coherent Vibrational Dynamics in Rigid PBI H-aggregates

Seongsoo Kang[1,3], Taeyeon Kim[1,3,4], Yongseok Hong[1], Frank Würthner[2], and Dongho Kim[1,]*

[1]Spectroscopy Laboratory for Functional π-Electronic Systems and Department of Chemistry, Yonsei University, Seoul 03722, South Korea

[2]Institut für Organische Chemie and Center for Nanosystems Chemistry, Universität Würzburg, Am Hubland, 97074 Würzburg, Germany

[3]S.K. and T.K. contributed equally.

[4]Current address: Department of Chemistry and Institute for Sustainability and Energy at Northwestern, Northwestern University, Evanston, Illinois 60208-3113 (United States)

AUTHOR INFORMATION

Corresponding Author

*E-mail for D.K.: dongho@yonsei.ac.kr

Table of Contents

Experimental details

1. Steady-state measurement

RM and **OM** were prepared according to the reported methods (see the main text). Steady-state absorption spectra were measured on a UV/Vis spectrometer (Varian, Cary5000) and photoluminescence spectra were measured on a fluorescence spectrophotometer (Hitachi, F-2500). Photoluminescence spectra are spectrally corrected by using correction factor of the fluorescence spectrophotometer. Anhydrous-grade solvents were purchased from Sigma-Aldrich and used without further purification. All steady-state measurements carried out by using a quartz cuvette with a pathlength of 1 cm at ambient temperatures.

2. Ground-state Raman measurements

Ground-state non-resonant Raman spectrum of **OA** was measured by using a Raman microscope (LabRam Aramis, Horiba Jovin Yvon) with 660 nm diode laser. For ground-state Raman measurements in reduced **OA**, first reduction potential (-0.8 V) is obtained by CV measurements using a CHI621D potentiostat (CH Instruments, Inc.) with a Pt working electrode, a Pt wire counter electrode and a 0.1 M Ag/AgCl reference electrode. The **OA** solution with an electrolyte consisting of anhydrous tetrahydrofuran (≥99.8%, Sigma-Aldrich) and 0.1 M $TBAPF_6$ (Tetrabutylammonium hexafluorophosphate, for electrochemical analysis, ≥99.0%, Sigma-Aldrich) was put in a CaF_2 windows with a pathlength of 200 μm at ambient temperatures.

3. Femtoseconds transient absorption measurements

The femtosecond transient absorption (fs-TA) spectrometer consists of an optical parametric amplifier (OPA; Palitra, Quantronix) pumped by a Ti:sapphire regenerative amplifier system (Integra-C, Quantronix) operating at 1 kHz repetition rate and an optical detection system. The generated OPA pulses have a pulse width of ~ 200 fs in the range of 280-2700 nm, which are used as pump pulses. White light continuum (WLC) probe pulses were generated using a sapphire window (4 mm thick) and a YAG window (4 mm thick) by focusing a small portion of the fundamental 800 nm pulses which was picked off by a quartz plate before entering the OPA. The time delay between pump and probe beams was carefully controlled by making the pump beam travel along a variable optical delay (ILS250, Newport). Intensities of the spectrally dispersed WLC probe pulses are monitored by a High Speed Spectrometer (Ultrafast Systems) for both visible and near-infrared measurements. To obtain the time-resolved transient absorption difference signal (ΔA) at a specific time, the pump pulses were chopped at 500 Hz and absorption spectra intensities were saved alternately with or without pump pulse. Typically, 4000 pulses excite the samples to obtain the fs-TA spectra at each delay time. The polarization angle between pump and probe beam was set at the magic angle (54.7°) using a Glan-laser polarizer with

a half-wave retarder in order to prevent polarization-dependent signals. Cross-correlation fwhm in pump-probe experiments was around 200 fs and chirp of WLC probe pulses was measured to be 1.2 ps in the 450-800 nm region. To minimize chirp, all reflection optics were used in the probe beam path. A quartz cell of 2 mm path length was employed. After completing each set of TA experiments, the absorption spectra of all samples were carefully checked to rule out the presence of artifacts or spurious signals arising from, for example, degradation or photo-oxidation of the samples in question.

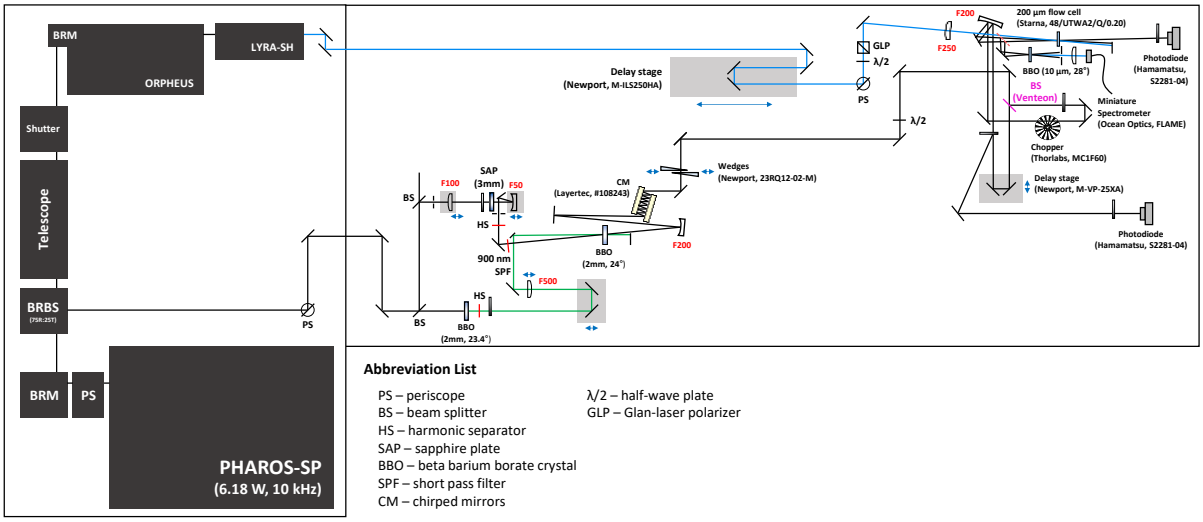

Figure S1. Schematic diagram of the TR-ISRS setup.

4. Time-resolved impulsive stimulated Raman spectroscopy (TR-ISRS)

A schematic diagram of the TR-ISRS is shown in Figure S1. We built and modified the setup by referring to papers from Tahara, Kukura, Brida, Ruhman, and Nelson groups.[1–7]

For the TR-ISRS setup, we use a Yb:KGW regenerative amplifier (PHAROS-SP-1.5mJ, Light Conversion, 1030 nm, 170 fs, 1.5 mJ, 10 kHz). First, a fundamental pulse passes through a periscope and then it is divided into two pulses by a 7(R):3(T) beam splitter. A smaller portion of the fundamental pulse (~ 1.55 W, 155 μJ) enters to a commercial collinear optical parametric amplifier (OPA) system (ORPHEUS, Light Conversion) combined with a second-harmonic-generation stage (LYRA-SH, Light Conversion), which allow us to get easy and broad tunability of an actinic pump pulse (P1). The pulse duration of OPA output is about 200 fs. A larger portion of the fundamental pulse (~ 4.63 W, 463 μJ) passes through a periscope (horizontal polarization → vertical polarization) and is additionally divided into two pulses by a 1(R):9(T) beam sampler (Newport) to generate a one-stage home-built non-collinear optical parametric amplifier (NOPA). A white-light seed pulse (generated in a 3-mm-thick sapphire plate (c-axis cut, Eksma optics)) and a second harmonics (515 nm, 40 μJ) of the fundamental pulse (generated in a 2-mm-thick BBO crystal (type 1, theta = 23.4°, Eksma optics)) are spatially and temporally overlapped in a 2-mm thick BBO crystal (type 1, theta = 24°, Eksma optics), which generates a highly stable (short-term: 0.3-0.5% rms fluctuation, long-term: > 48 hrs) broadband near-infrared (NIR) NOPA centered at 800 nm (Figure S2b, see below). Pulse compression of the NIR-NOPA output is carried out by using a pair of chirped mirrors (#108243, Layertec) and wedges (23RQ12-02-M). We carefully determined the number of bounces (7 bounces/mirror) on the chirped mirrors and thicknesses at certain position of the wedges considering additional chirps after the pulse compression stage (by a half-wave plate, a neutral density filter, a beam splitter and a sample window). The pulse duration of the compressed NIR-NOPA output is determined to be 9.5 fs, which is retrieved by second harmonic generation frequency resolved optical gating (SHG-FROG) in a 10 μm BBO crystal (type 1, theta = 28°, Eksma optics) (Figure S2a).[8] In order to prepare Raman pump (P2) and probe (P3) pulses, the compressed NIR-NOPA is divided into two by a 1(R):1(T) beam splitter (Venteon). In particular, we do not need to use additional compensation plate for the reflected pulse owing to specially designed broadband dielectric coating that makes the group delay dispersion (GDD) of the transmitted and reflected pulses identical. The delay times, T (the time interval between the P1 and P2 pulses) and τ (the time interval between the P2 and P3 pulses), are controlled by the motorized linear stages (M-ILS250HA (Newport) and M-VP-25XA (Newport) for T and τ, respectively). In the probe beamline, a small portion of NOPA reflected from the neutral density filter (variable, reflective-type, NDC-50S-1, Thorlabs) is used as the reference pulse for balanced detection. The P1 pulse and the P2/P3 pulses are focused by a plano-convex lens (f = 250 mm) and a concave mirror (f = 200 mm), respectively. At the focal point, beam diameters (1/e2) of the P1 (490 nm, 150 nJ), P2 (800 nm, 80 nJ), and P3 (800 nm, 8 nJ) pulses are 160, 120, and 100 μm, respectively. Polarization of all three pulses are parallel (horizontally polarized) at the sample position. In order to minimize GDD, we use an ultrathin wall aperture (200 μm-

thick UVFS) flow cell (48/UTWA2/Q/0.2, Starna) with 200 μm optical path length. Also, a micro annular gear pump (mzr-4622 M2.1) with Teflon tubing is used for flowing the sample solutions which can remove the thermal-lens effect due to the 10 kHz repetition rate of the laser and avoiding photo-degradation of the sample. We usually prepare 2–3 ml sample solutions for the experiments. The optical densities at 510 nm for **RM** and **RO** in chloroform, and at 490 nm for **RA** and **RO** in MCH are ~0.7 in the 200 μm path length cell.

The P3 and the reference pulses are detected using the Si photodiodes (S2281-04, Hamamatsu) without the color or band-pass filters for open-band (non-dispersive) detection in order to minimize the vibrational coherences from the ground-state of the sample and solvent. For the details of the open-band detection, please refer to ref 2. The input signals are first amplified by a low-noise current preamplifier (SR570, Stanford Research Systems) and then the peak voltages of every laser shot are recorded by a data acquisition (DAQ) card (NI-PCI-6220, National Instruments) with setting a sampling rate of 10000/sec. The P2 pulse is modulated at 5 kHz by a mechanical chopper (MC1F60, Thorlabs), which allows data processing in a shot-to-shot fashion.

It has been known that sample treatment is one of the most decisive part in the TR-ISRS experiments. Even though we prepared highly stable laser pulses, if there are particles and/or bubbles (even after performing filtration processes) in sample solutions, the spike signals can be detected in raw TR-ISRS kinetic profiles.[2] Even the kinetic profiles that contain a single spike can induce a significant noise in the Raman spectra after performing Fourier transformation analysis.[2] Therefore, we have adopt a pre-processing procedure, trimmed mean", to eliminate the spike signals immediately in a τ scan before averaging the data. For example, in order to measure one data point at certain delay time (τ), we averaged 12 pre-averaged TA signals, where each pre-averaged TA signal (-log(IP2,ON/IP2,OFF)) is obtained by averaging 250 TA signals calculated from 250 pairs of laser shots (250 pulses for IP2,ON and the other 250 pulses for IP2,OFF). Among the calculated 250 TA signals, the spikes correspond to a small number of outliers deviated from the real average value, so we first trimmed 10% from the 250 TA signals. The lowest 10% (25 TA signals) and the highest 10% (25 TA signals) were discarded and we computed the mean of the remaining 80% (200 TA signals calculated from 400 pulses). Subsequently, as some strong spike signals can still remain unexpectedly, so we additionally trimmed 10% from the twelve pre-averaged TA signals. As a result, one data point at certain delay time in the TR-ISRS kinetic profiles is obtained by averaging TA signals calculated from 2000 pairs (200 pairs x 10) of the laser shots. In our experience, by performing two consecutive "trimmed mean" procedures can eliminate the unwanted spike signals entirely, so we do not need any post-processing to remove the spikes manually.

The pump pulse is modulated at 5 kHz by a mechanical chopper (MC1F60, Thorlabs), which allows data processing in a shot-to-shot fashion. 30000x2 pulses are averaged for each time delay and its effect for enhancing the data quality is represented in Figure S3. As a reference, neat acetonitrile is measured, as shown in Figure S4.

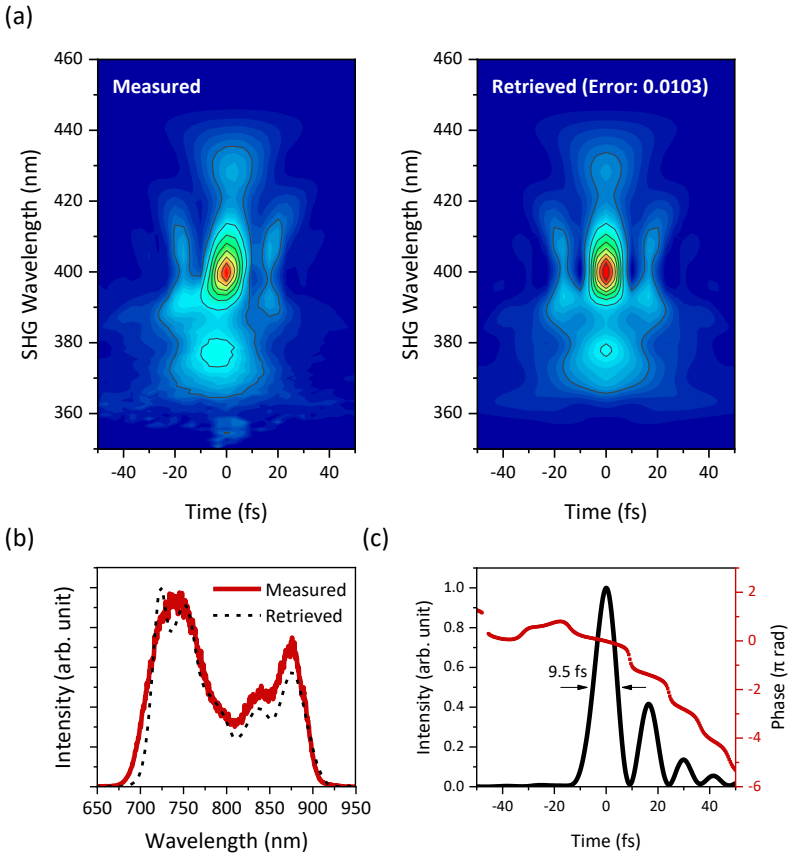

Figure S2. (a) Measured (left) and the retrieved (right) SHG-FROG traces, (b) comparison between the NIR-NOPA spectrum and the SHG-FROG retrieved spectrum, and (c) retrieved intensity and phase profiles of the NIR-NOPA.

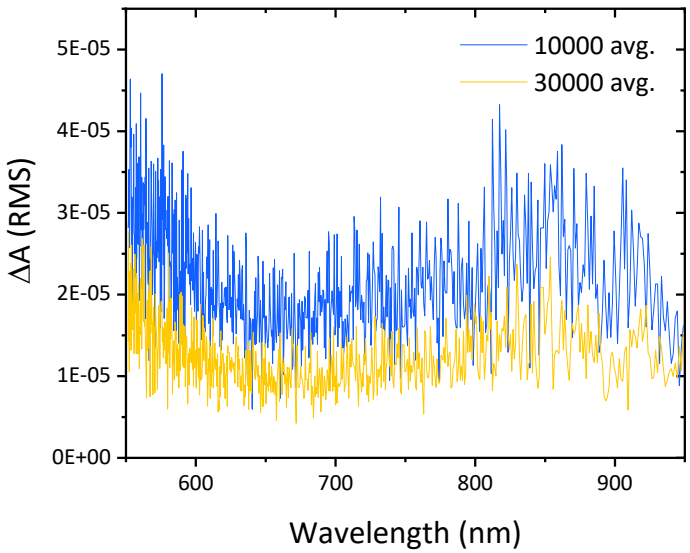

Figure S3. Probe pulse stability. Pulse fluctuation (root mean square fluctuation) at each wavelength when averaging 10000 and 30000 shots.

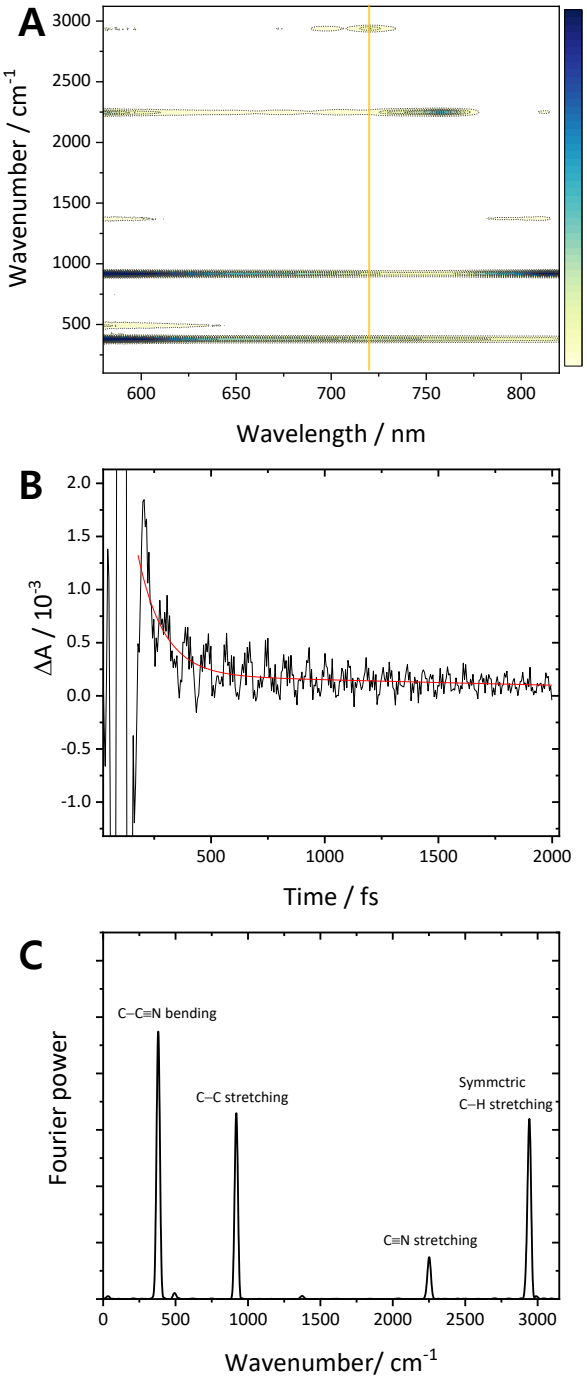

Figure S4. Non-resonant impulsive stimulated Raman scattering (ISRS) measurements on acetonitrile. (A) Fourier power map of acetonitrile (ACN). (B) Raw time-domain signal at 720 nm (yellow line in (**a**)) with a fitting line (red). (C) Fourier power spectrum at this wavelength where Fourier transform is performed on residual time-domain sginal after windowing (Hanning window) and zero-padding.

5. Vibrational coherence measurements by ultrafast TA

A schematic diagram of our newly constructed ultrafast transient absorption (TA) setup is shown in Figure S5. We built and modified the setup by referring to papers from Tahara, Kukura, Brida, Ruhman, and Nelson groups.[1-7] For the ultrafast TA setup, we use a Yb:KGW regenerative amplifier (PHAROS-SP-1.5mJ, Light Conversion, 1030 nm, 170 fs, 1.5 mJ, 10 kHz). 7 fs visible home-built noncollinear parametric amplifier (VIS-NOPA) pulse is generated at BBO by overlapping 343 nm third-harmonic generation (THG) pump and seed pulse (white light continuum). Vis-NOPA is compressed via chirped mirrors where pre-compression before BBO and post-compression after BBO followed by fine-tuning with the wedge prism pair and its temporal width reaches 7 fs as shown in Figure S6. The delay time is controlled by the motorized linear stage (M-VP-25XA (Newport)). Polarizations of two pulses are parallel at the sample position. The signals are obtained by a CCD detector (Stresing, FL-3030). In order to minimize GDD, we use an ultrathin wall aperture (200 μm UVFS) flow cell (48/UTWA2/Q/0.2, Starna) with 200 μm optical path length. Also, a micro annular gear pump (mzr-4622 M2.1) with Teflon tubing is used for flowing the sample solutions which can remove the thermal-lens effect due to the 10 kHz repetition rate of the laser and avoid photo-degradation of the sample. We usually prepare 2–3 ml sample solutions for the experiments.

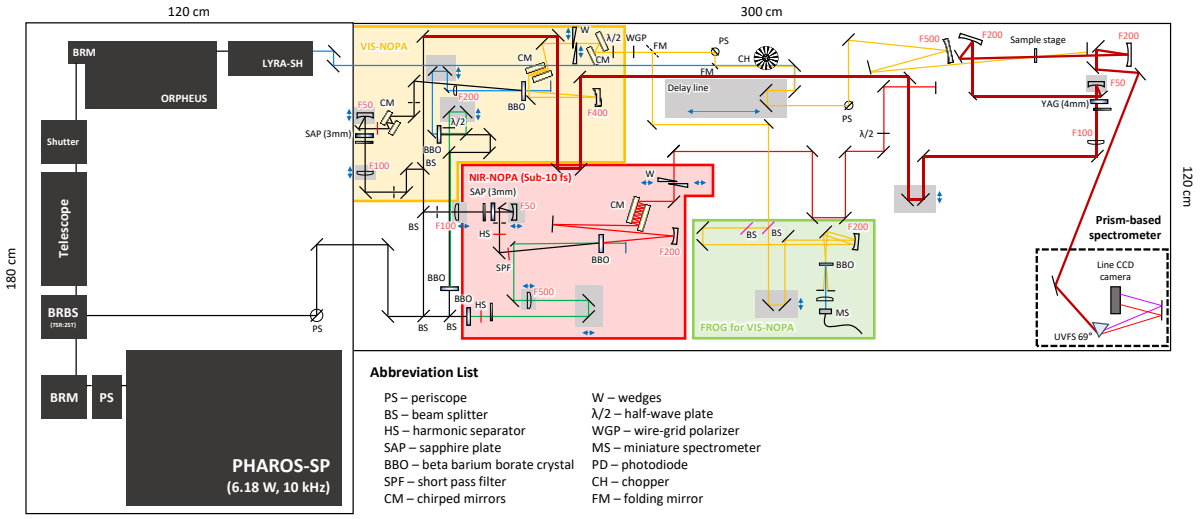

Figure S5. Ultrafast TA setup Schematic diagram of transient absorption setup using VIS- or NIR-NOPA as the pump and white light continuum as the probe.

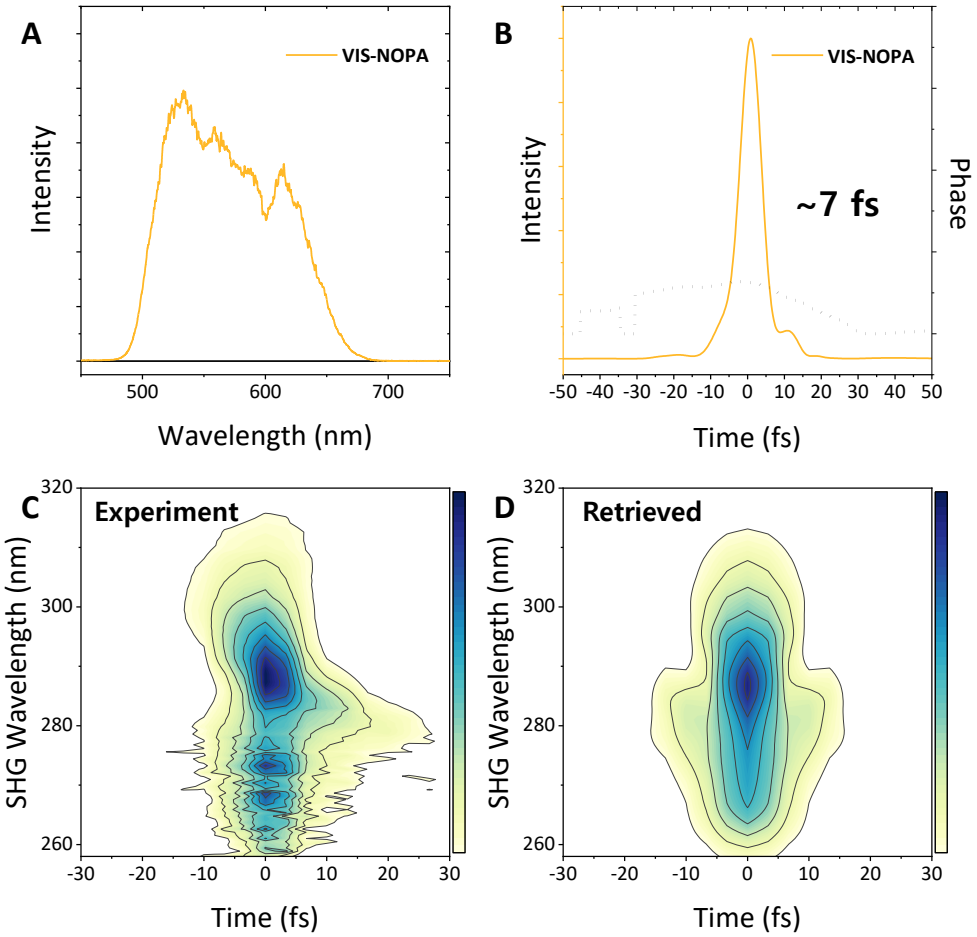

Figure S6. VIS-NOPA pulse characterization (A) VIS-NOPA spectrum (B) temporal profile of VIS-NOPA and phase. (C) Measured and the (D) retrieved SHG-FROG traces.

6. Quantum mechanical calculations

Quantum mechanical calculations were carried out with Gaussian 16 program suite.[9] All calculations (DFT and TD-DFT) were performed based on CAM-B3LYP employing a basis set consisting of 6-31+G(d,p) for all atoms.[10] Dodecyl chains on tridodecylphenly (TDP) and tridodecyloxyphenyl (TDOP) groups of **RM** and **RO** were replaced by methyl groups to reduce computational cost, respectively. Additionally, for H-dimer models of **RA** and **OA**, empiricaldispersion=gd3 is used to consider deispersion interaction in the aggregates.[11]

7. Simulation of absorption spectra according to the exciton coupling strength

By using the single-particle approximation (SPA) for simulating absorption spectra by Spano et al., the excitonic coupling strength of **RA** and **OA** is obtained by comparison of the measured absorption spectra in MCH with the theoretical model.[12-14] To simulate the absorption spectra, the Huang-Rhys (HR) factor of **RM** and **OM** in CF is used and fitted in 0.65 and 0.66, respectively.

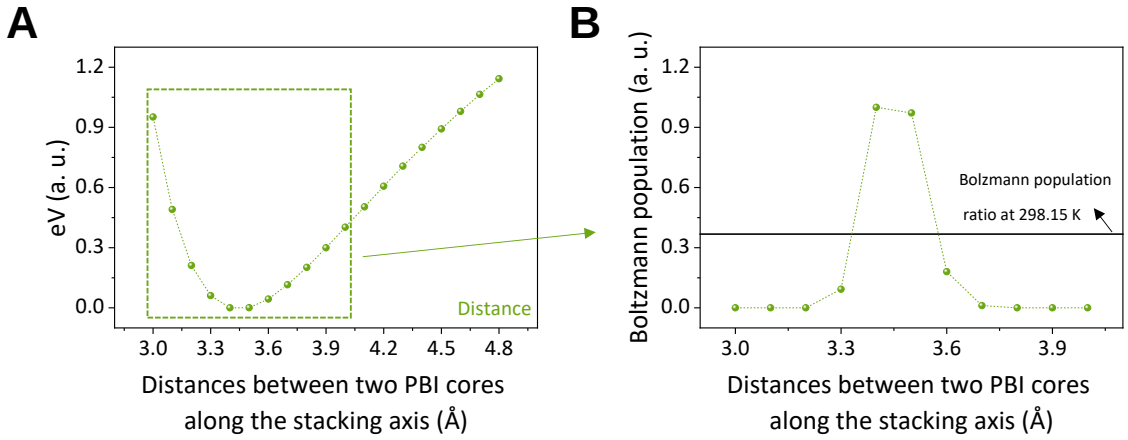

Figure S7. Relative potential energy plot of PBI-OR dimer as a function of the distance between PBI cores with fixed angle at 30 degree (A) and Boltzmann distribution of populations at room-temperature (298.15 K). Each energy at fixed distances was obtained by the single point calculations.

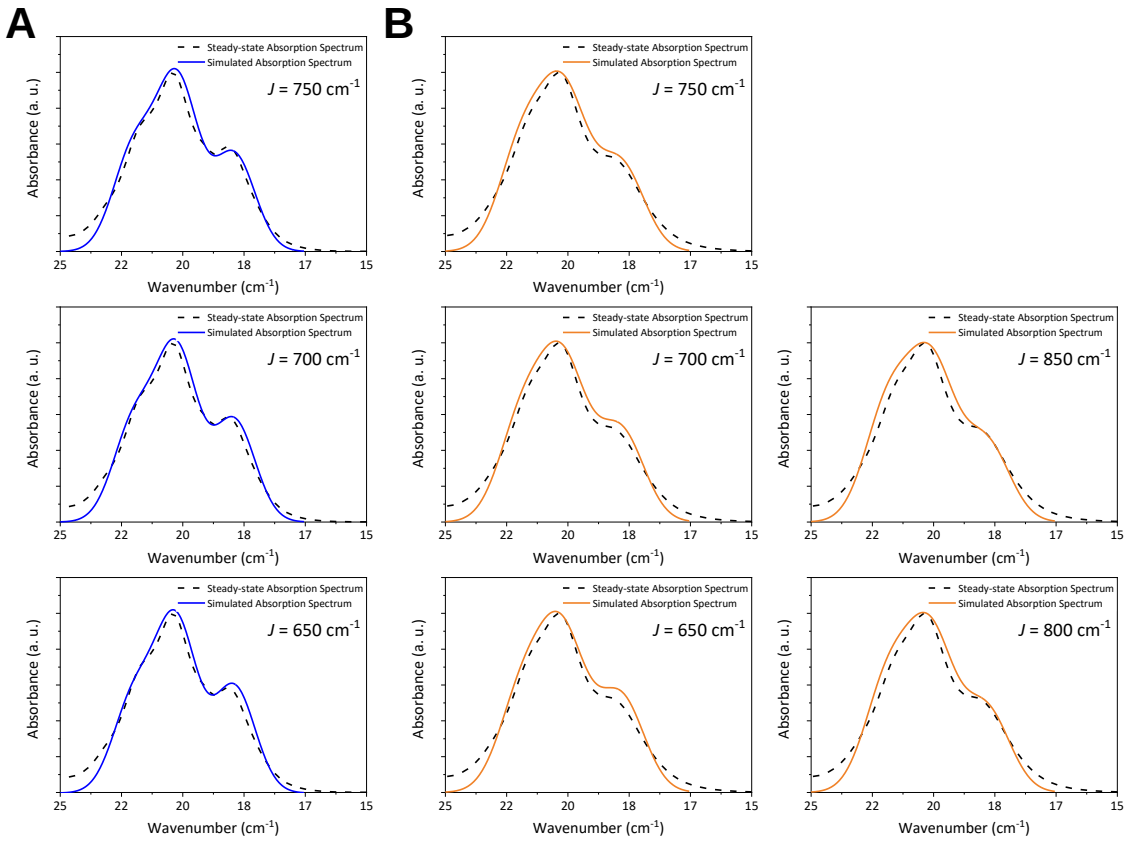

Figure S8. Calculated (colored) and the measured (dashed) absorption spectra of **RA** (blue) (A) and **OA** (orange) (B) varying the coupling strength (*J*) (The widths of vibronic bands were equally shared in the simulation).

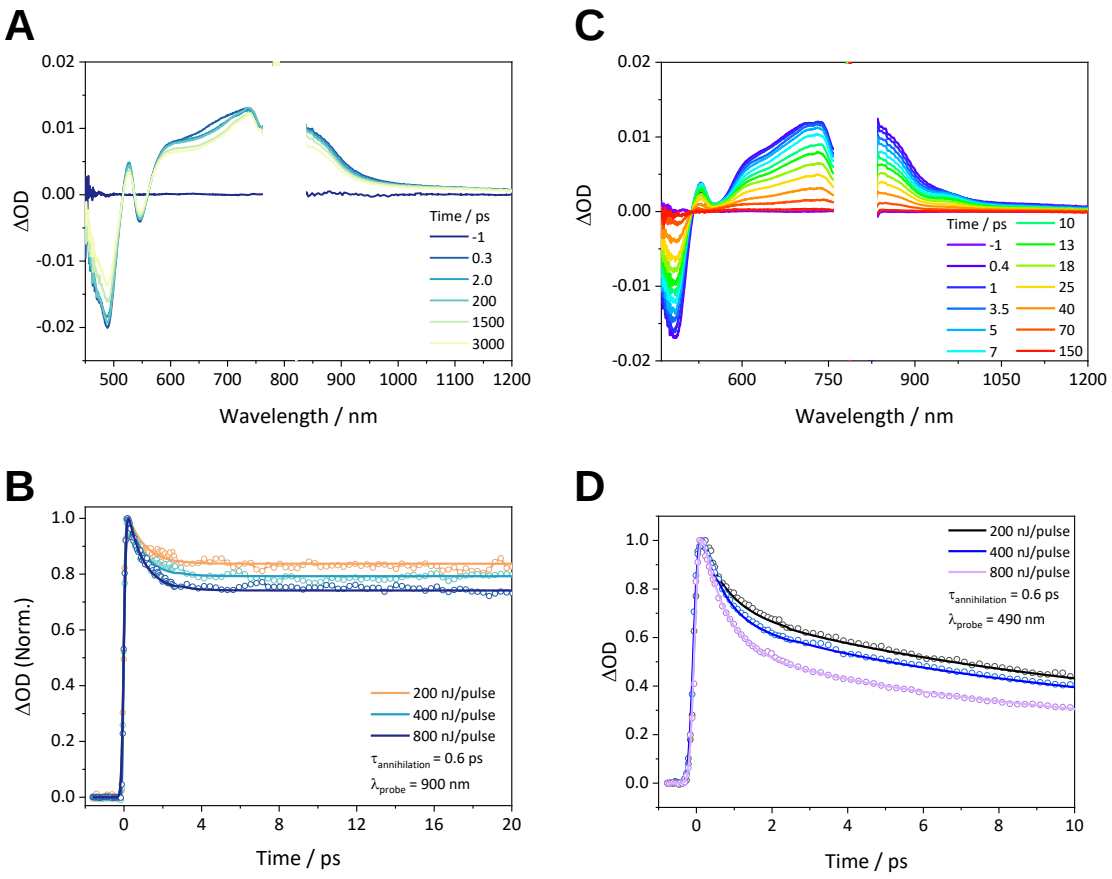

Figure S9. Femtosecond transient absorption spectra and pump-fluence dependent decay profiles in (A and B) **RA** and (C and D) **OA** in MCH, respectively. The excitation source at 490 nm is used.

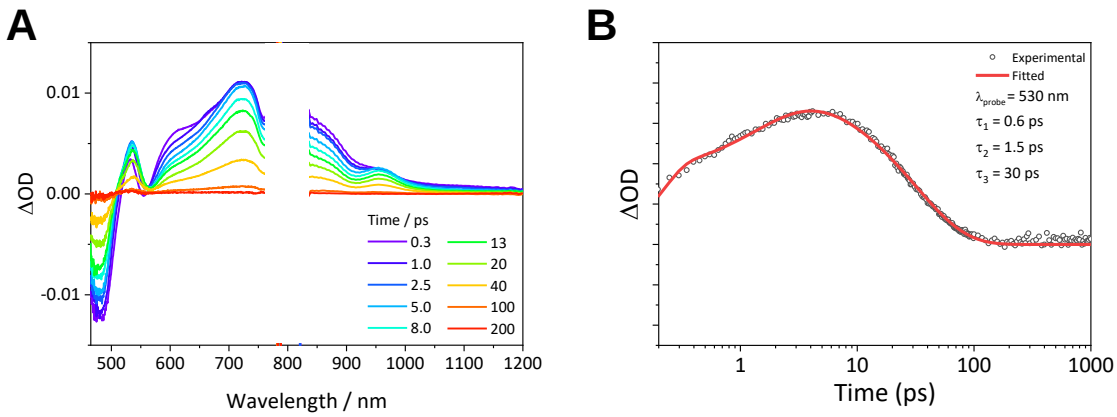

Figure S10. (A) Femtosecond transient absorption spectra and (B) decay profiles probed at 530 nm in **OA** in tetrahydrofuran (THF) ($\lambda_{excitation}$ = 490 nm).

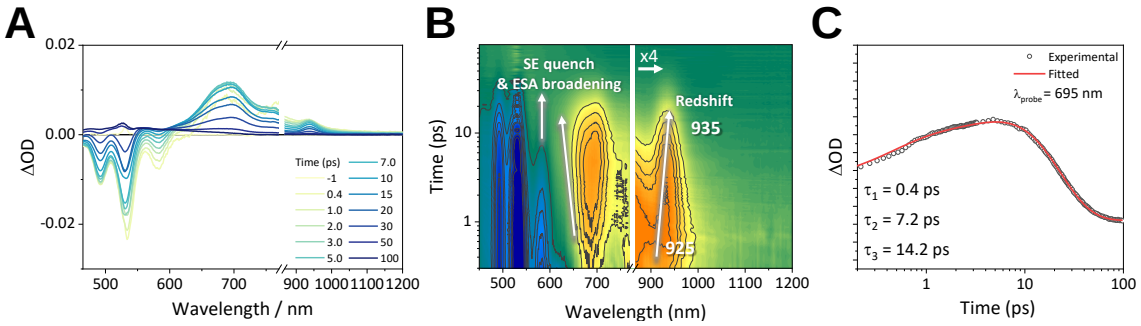

Figure S11. Femtosecond transient absorption (A) and 2D (B) spectra and decay profiles probed at 695 nm (C) in **OM** in highly diluted toluene (< 10^{-8} M), respectively. The excitation source at 530 nm is used. (Note that PBI-OR shows very large aggregate constants of the order of ~10^{7} in MCH, so PBI-OR monomer in MCH is not accessible in the scope of this work.)

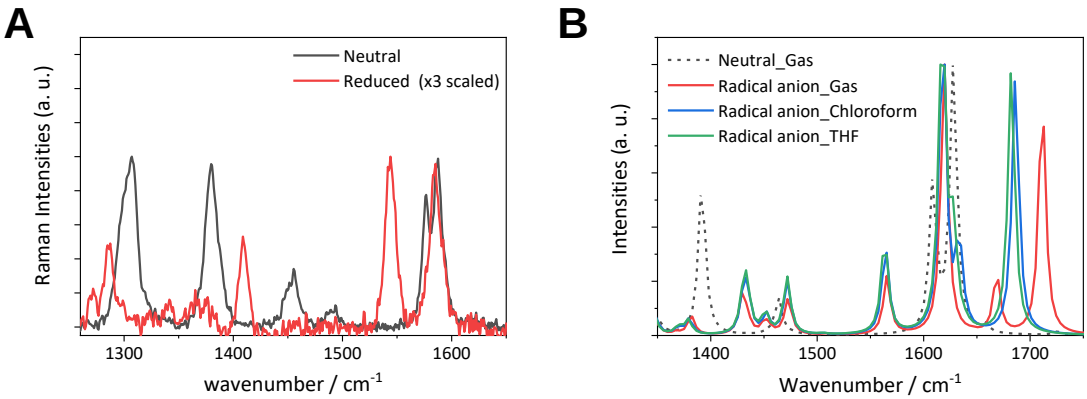

Figure S12. (A) Ground-state Raman spectra in neutral (black) and reduced (red) **OA** in THF. (B) Calculated Raman modes in neutral **OM** and reduced **OM** where the calculations were performed at CAM-B3LYP/6-31+G(d,p) by using the PCM model with solvent, chloroform and THF.

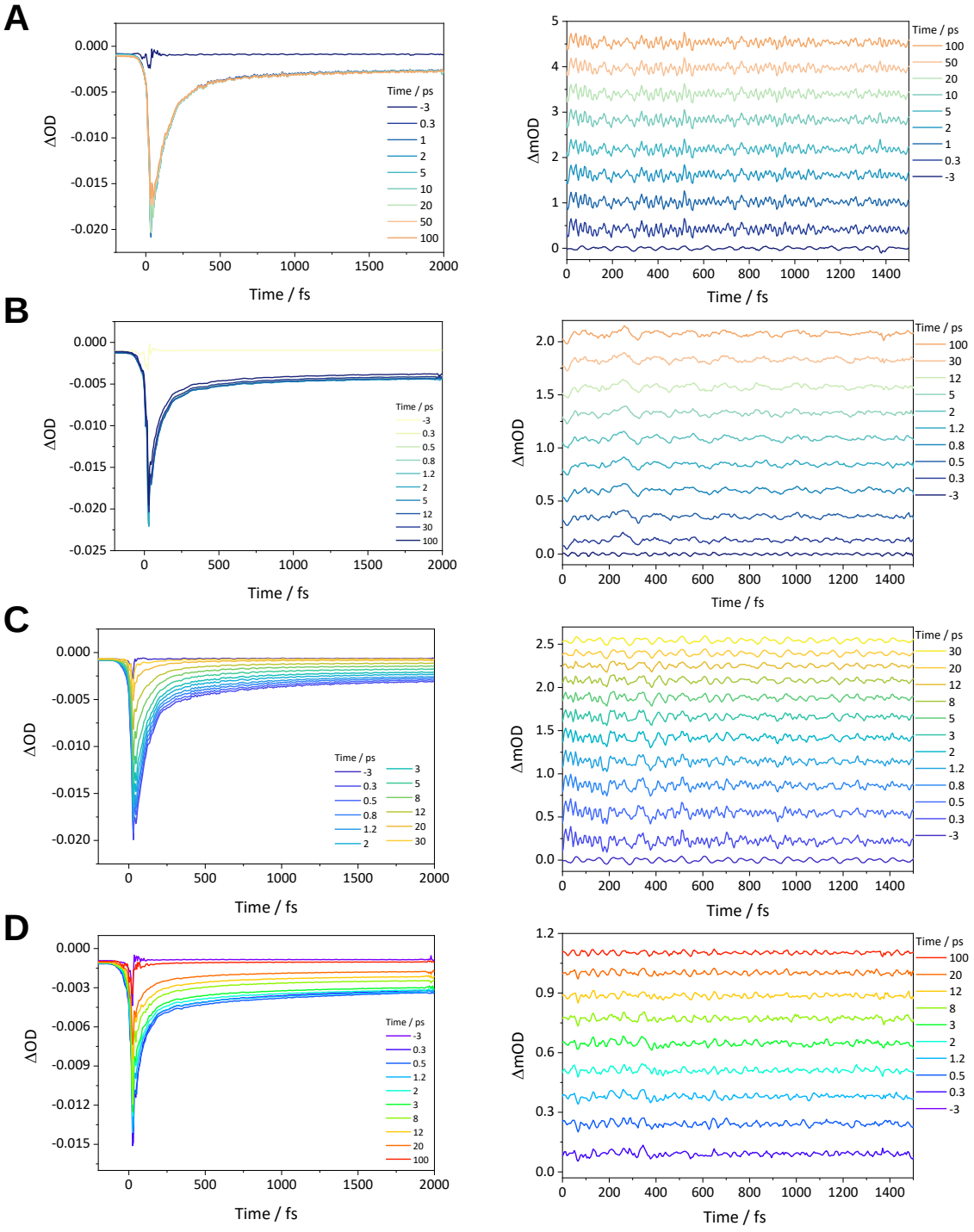

Figure S13. (A-D, left) Raw TR-ISRS signals of **RM** in chloroform, **RA** in MCH, **OM** in chloroform, and **OA** in MCH at particular delay times T and (A-D, right) oscillatory residuals extracted from multiexponential fits to the kinetic traces at each T, respectively.

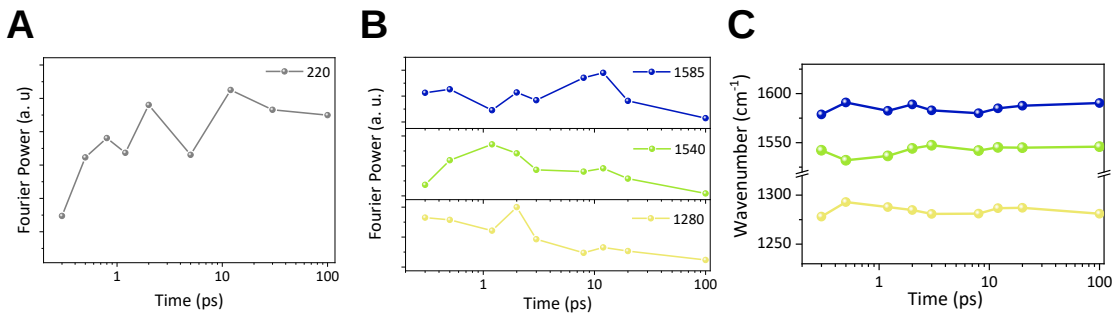

Figure S14. (A) Fourier Power intensity profiles at 220 cm^{-1} at the probed delay times T in **RA** (B) Fourier Power intensity profiles at 1585 (blue), 1540 (green), and 1280 (yellow) cm^{-1} modes at the probed delay times T and (C) the spectrally stationary Raman frequency profiles where the peak positions were determined by fitting each frequency mode to a Gaussian function in **OA**.

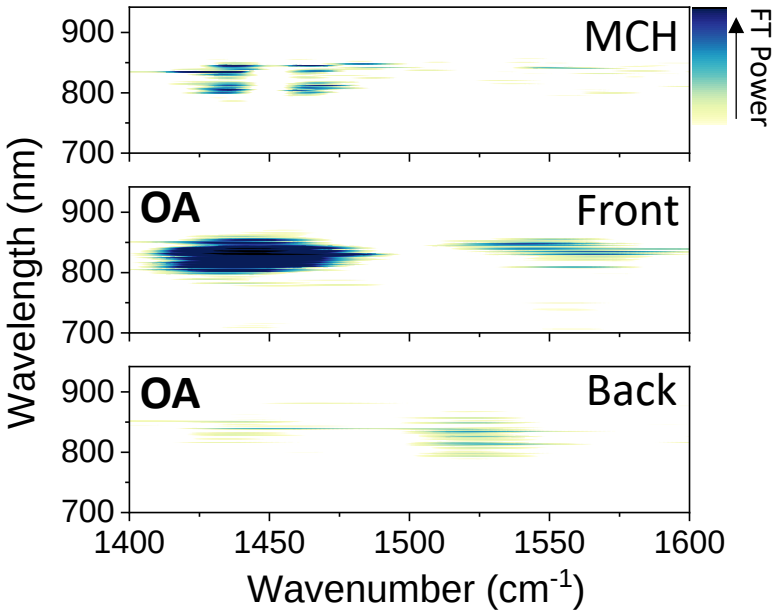

Figure S15. Fourier power contour maps of MCH solvent and **OA** by broadband TA measurements with ultrashort pump source of sub-10 fs vis-NOPA where excited-state wavepackets at 0-1 ps (front) and 1-2 ps (back) time windows are separately extracted to clarify the emerging Raman modes in the region of 1500-1550 cm^{-1}.

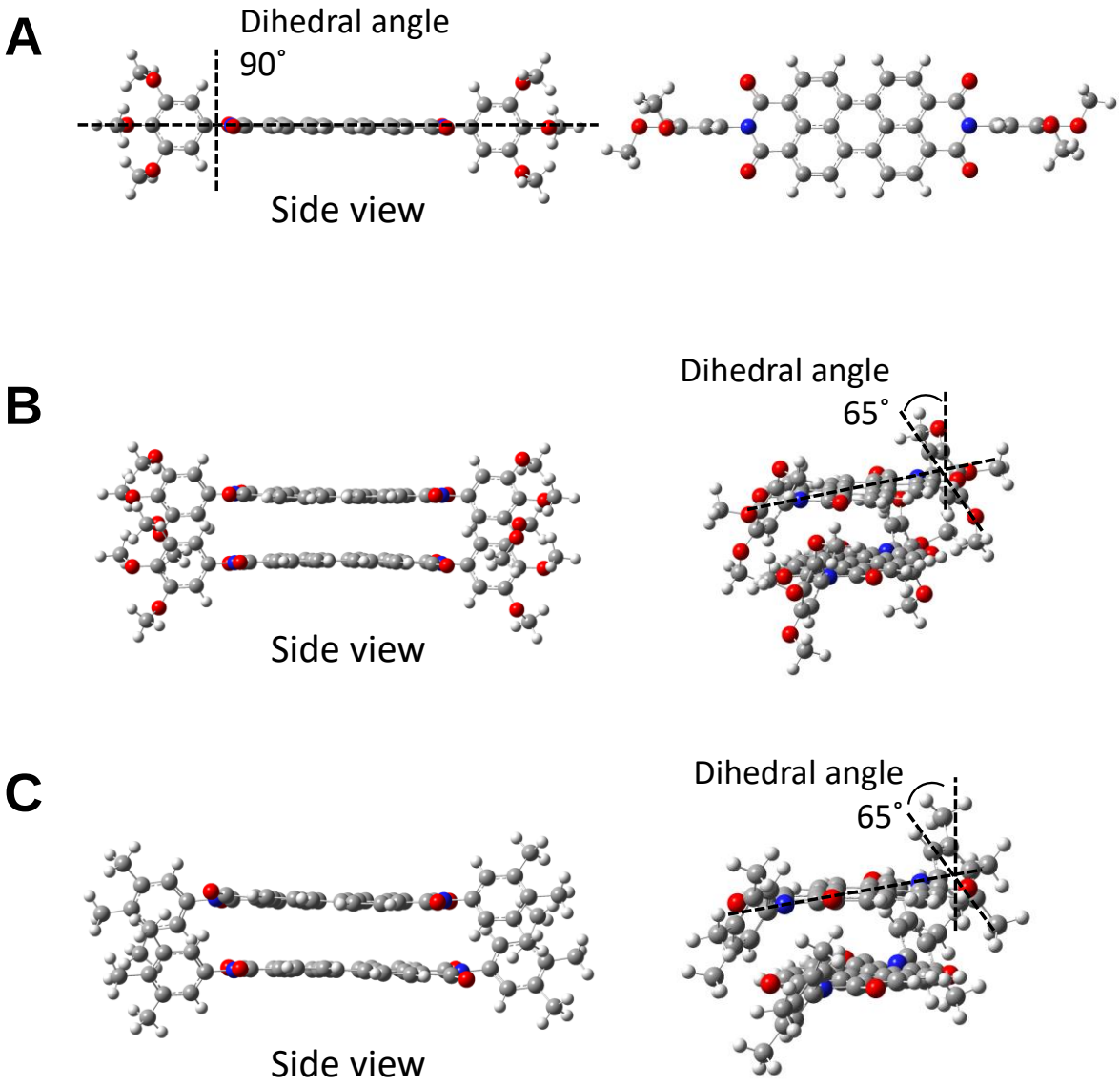

Figure S16. The geometry-optimized molecular structure (CAM-B3LYP/6-31+G(d,p)) in (A) **OM**. (B) **OA** H-dimer, and (C) **RA** H-dimer.

Reference

(1) Werley, C. A.; Teo, S. M.; Nelson, K. A. Pulsed Laser Noise Analysis and Pump-Probe Signal Detection with a Data Acquisition Card. *Rev. Sci. Instrum.* **2011**, *82* (12).

(2) Kuramochi, H.; Takeuchi, S.; Tahara, T. Femtosecond Time-Resolved Impulsive Stimulated Raman Spectroscopy Using Sub-7-Fs Pulses: Apparatus and Applications. *Rev. Sci. Instrum.* **2016**, *87* (4).

(3) Liebel, M.; Schnedermann, C.; Wende, T.; Kukura, P. Principles and Applications of Broadband Impulsive Vibrational Spectroscopy. *J. Phys. Chem. A* **2015**, *119* (36), 9506–9517.

(4) Grupp, A.; Budweg, A.; Fischer, M. P.; Allerbeck, J.; Soavi, G.; Leitenstorfer, A.; Brida, D. Broadly Tunable Ultrafast Pump-Probe System Operating at Multi-KHz Repetition Rate. *J. Opt. (United Kingdom)* **2018**, *20* (1).

(5) Liebel, M.; Schnedermann, C.; Kukura, P. Sub-10-Fs Pulses Tunable from 480 to 980 Nm from a NOPA Pumped by an Yb:KGW Source. *Opt. Lett.* **2014**, *39* (14), 4112.

(6) Banin, U.; Kosloff, R.; Ruhman, S. Vibrational Relaxation of Nascent Diiodide Ions Studied by Femtosecond Transient Resonance Impulsive Stimulated Raman Scattering (TRISRS); Experiment and Simulation. *Chem. Phys.* **1994**, *183* (2–3), 289–307. https://doi.org/10.1016/0301-0104(94)00099-9.

(7) Banin, U.; Ruhman, S. Ultrafast Vibrational Dynamics of Nascent Diiodide Fragments Studied by Femtosecond Transient Resonance Impulsive Stimulated Raman Scattering. *J. Chem. Phys.* **1993**, *99* (11), 9318–9321. https://doi.org/10.1063/1.465501.

(8) Trebino, R.; DeLong, K. W.; Fittinghoff, D. N.; Sweetser, J. N.; Krumbügel, M. A.; Richman, B. A.; Kane, D. J. Measuring Ultrashort Laser Pulses in the Time-Frequency Domain Using Frequency-Resolved Optical Gating. *Rev. Sci. Instrum.* **1997**, *68* (9), 3277–3295.

(9) Frisch, M. J. et al. Gaussian 16, Revision C.01, Gaussian, Inc., Wallingford CT 2016.

(10) Katari, M.; Nicol, E.; Steinmetz, V.; van der Rest, G.; Carmichael, D.; Frison, G. Improved Infrared Spectra Prediction by DFT from a New Experimental Database. *Chem. - A Eur. J.* **2017**, *23* (35), 8414–8423.

(11) Grimme, S.; Antony, J.; Ehrlich, S.; Krieg, H. A Consistent and Accurate Ab Initio Parametrization of Density Functional Dispersion Correction (DFT-D) for the 94 Elements H-Pu. *J. Chem. Phys.* **2010**, *132* (15).

(12) Spano, F. C. Modeling Disorder in Polymer Aggregates: The Optical Spectroscopy of Regioregular Poly(3-Hexylthiophene) Thin Films. *J. Chem. Phys.* **2005**, 122 (23). https://doi.org/10.1063/1.1914768.

(13) Spano, F. C.; Yamagata, H. Vibronic Coupling in J-Aggregates and beyond: A Direct Means of Determining the Exciton Coherence Length from the Photoluminescence Spectrum. *J. Phys. Chem. B* **2011**, 115 (18), 5133–5143.

https://doi.org/10.1021/jp104752k.

(14) Sung, J.; Kim, P.; Fimmel, B.; Würthner, F.; Kim, D. Direct Observation of Ultrafast Coherent Exciton Dynamics in Helical π-Stacks of Self-Assembled Perylene Bisimides. *Nat. Commun*. **2015**, 6. https://doi.org/10.1038/ncomms9646.